

ORIGINAL STUDIES

EDITORIAL COMMENT: Expert Article Analysis for:
FFR_{CT}: Getting better all the time (but not there yet)

Non-invasive procedural planning using computed tomography-derived fractional flow reserve

Michiel J. Bom MD¹ | Stefan P. Schumacher MD¹ | Roel S. Driessen MD¹  |
Pepijn A. van Diemen MD¹ | Henk Everaars MD¹ | Ruben W. de Winter MD¹ |
Peter M. van de Ven PhD² | Albert C. van Rossum MD PhD¹ |
Ralf W. Sprengers MD PhD³ | Niels J.W. Verouden MD PhD¹ |
Alexander Nap MD PhD¹ | Maksymilian P. Opolski MD PhD^{1,4} |
Jonathon A. Leipsic MD⁵ | Ibrahim Danad MD PhD¹ | Charles A. Taylor PhD^{6,7} |
Paul Knaapen MD PhD¹ 

¹Amsterdam UMC, Vrije Universiteit Amsterdam, Department of Cardiology, Amsterdam Cardiovascular Sciences, Amsterdam, The Netherlands

²Amsterdam UMC, Vrije Universiteit Amsterdam, Department of Epidemiology and Biostatistics, Amsterdam, The Netherlands

³Amsterdam UMC, Vrije Universiteit Amsterdam, Department of Radiology & Nuclear Medicine, Amsterdam, The Netherlands

⁴Department of Interventional Cardiology and Angiology, Institute of Cardiology, Warsaw, Poland

⁵Department of Medicine and Radiology, University of British Columbia, Vancouver, British Columbia, Canada

⁶HeartFlow, Inc, Redwood City, California

⁷Department of Bioengineering, Stanford University, Stanford, California

Correspondence

Paul Knaapen, Amsterdam UMC, Vrije Universiteit Amsterdam, Department of Cardiology, Amsterdam Cardiovascular Sciences, De Boelelaan 1118, 1081 HZ, Amsterdam.
Email: p.knaapen@vumc.nl

Abstract

Objectives: This study aimed to investigate the performance of computed tomography derived fractional flow reserve based interactive planner (FFR_{CT} planner) to predict the physiological benefits of percutaneous coronary intervention (PCI) as defined by invasive post-PCI FFR.

Background: Advances in FFR_{CT} technology have enabled the simulation of hyperemic pressure changes after virtual removal of stenoses.

Methods: In 56 patients (63 vessels) invasive FFR measurements before and after PCI were obtained and FFR_{CT} was calculated using pre-PCI coronary CT angiography. Subsequently, FFR_{CT} and invasive coronary angiography models were aligned allowing virtual removal of coronary stenoses on pre-PCI FFR_{CT} models in the same locations as PCI was performed. Relationships between invasive FFR and FFR_{CT}, between post-PCI FFR and FFR_{CT} planner, and between delta FFR and delta FFR_{CT} were evaluated.

Results: Pre PCI, invasive FFR was 0.65 ± 0.12 and FFR_{CT} was 0.64 ± 0.13 ($p = .34$) with a mean difference of 0.015 (95% CI: -0.23 – 0.26). Post-PCI invasive FFR was 0.89 ± 0.07 and FFR_{CT} planner was 0.85 ± 0.07 ($p < .001$) with a mean difference of 0.040 (95% CI: -0.10 – 0.18). Delta invasive FFR and delta FFR_{CT} were 0.23 ± 0.12 and 0.21 ± 0.12 ($p = .09$) with a mean difference of 0.025 (95% CI: -0.20 – 0.25). Significant correlations were found between pre-PCI FFR and FFR_{CT} ($r = 0.53$, $p < .001$), between post-PCI FFR and FFR_{CT} planner ($r = 0.41$, $p = .001$), and between delta FFR and delta FFR_{CT} ($r = 0.57$, $p < .001$).

This is an open access article under the terms of the Creative Commons Attribution-NonCommercial License, which permits use, distribution and reproduction in any medium, provided the original work is properly cited and is not used for commercial purposes.

© 2020 The Authors. *Catheterization and Cardiovascular Interventions* published by Wiley Periodicals LLC.

Conclusions: The non-invasive FFR_{CT} planner tool demonstrated significant albeit modest agreement with post-PCI FFR and change in FFR values after PCI. The FFR_{CT} planner tool may hold promise for PCI procedural planning; however, improvement in technology is warranted before clinical application.

KEYWORDS

computed tomography derived fractional flow reserve, coronary artery disease, coronary computed tomography angiography, fractional flow reserve, percutaneous coronary intervention

1 | INTRODUCTION

Coronary revascularization with percutaneous coronary intervention (PCI) aims to relieve myocardial ischemia caused by a coronary stenosis through augmenting coronary flow and myocardial perfusion. Fractional flow reserve (FFR), calculated as the pressure ratio across a coronary stenosis during maximal hyperemia, is regarded the gold standard for the detection of lesion-specific ischemia and is used to guide revascularization.¹ Furthermore, post-PCI FFR provides important insight into the restoration of perfusion following revascularization, given the close correlation between post-PCI FFR and absolute myocardial blood flow measured with positron emission tomography.² FFR values and changes in FFR following PCI have also been linked with adverse events, demonstrating the importance of FFR to predict outcome after stenting.³⁻⁸ Over the last few years, FFR derived from computed tomography (FFR_{CT}) has emerged as a non-invasive alternative to invasive FFR. In FFR_{CT} computational fluid dynamics are used to assess coronary flow impairment across a coronary stenosis from standard coronary CT angiography (CTA) data.⁹ Several studies have demonstrated excellent diagnostic accuracy of FFR_{CT} when referenced by invasive FFR.¹⁰⁻¹² Recent advances in FFR_{CT} technology have led to the development of an FFR_{CT} -based interactive planner tool (FFR_{CT} planner) which enables the simulation of blood flow after virtual removal of a stenosis, hereby predicting the hemodynamic effects of stenting.^{13,14} The non-invasive prediction of the potential physiological benefit of stenting might be useful for PCI planning and lesion selection. This study therefore aimed to investigate the accuracy of FFR_{CT} planner to predict invasive post-PCI FFR and change in invasive FFR following PCI.

2 | MATERIALS AND METHODS

2.1 | Study population

This study is a combined substudy of the PACIFIC trial and the AR-PCI trial. The PACIFIC trial included consecutive patients with suspected coronary artery disease (CAD) who underwent coronary CTA, single photon emission computed tomography, and positron emission tomography, followed by invasive coronary angiography (ICA) with FFR measurement in all major coronary arteries regardless of non-invasive imaging findings.¹⁵ In patients in whom PCI was

performed, invasive FFR measurements were obtained after stenting. The AR-PCI trial was a randomized study on the effect of coronary CTA guided stenting versus angiography guided stenting in patients with a clinical indication for PCI (NCT03531424). Both studies included patients with stable CAD, without prior PCI in the target vessel. Both studies were approved by the Medical Ethics Committee of the VU University Medical Center and written informed consent was obtained from all participants.

2.2 | Coronary CTA acquisition

Patients underwent coronary CTA on a 256-slice CT-scanner (Brilliance iCT, Philips Healthcare, Best, the Netherlands) with a collimation of 128×0.625 mm and a tube rotation time of 270 ms. Tube current was set between 200 and 360 mAs at 120 kV, adjusting primarily mAs based on body habitus. Axial scanning was performed with prospective ECG-gating (Step & Shoot Cardiac, Philips Healthcare) at 75% of the R-R interval. A bolus of 100 ml iobitidol (Xenetix 350) was injected intravenously (5.7 ml/s) followed by a 50 ml saline flush. The scan was triggered using an automatic bolus tracking technique, with a region of interest placed in the descending thoracic aorta with a threshold of 150 Hounsfield Units (HU). In patients with a prescan heart rate of ≥ 65 beats per minute, metoprolol 50 to 150 mg was administered orally 1 hour before the start of the CT acquisition. If necessary, 5 to 25 mg metoprolol was given intravenously directly before the scan to achieve a heart rate < 65 bpm. All patients received 800 mcg of sublingual nitroglycerine immediately before scanning.

2.3 | FFR_{CT} analysis

FFR_{CT} was performed by HeartFlow Inc. (Redwood City, CA), blinded to angiographic and physiological data. FFR_{CT} is derived post hoc from standard coronary CTA data using previously described methodology.⁹ In short, it involves extraction of a patient specific geometric model of the coronary arteries, population-derived physiological models, and computational fluid dynamics techniques to solve the governing equations of blood flow for velocity and pressure under simulated hyperemic conditions. In the current study HeartFlow FFR_{CT} v2.7 was used, which comprises deep-learning artificial intelligence methods to aid in identifying the lumen boundary, physiological

models incorporating vessel lumen volume as well as myocardial mass data and hybrid 3-dimensional-1-dimensional computational fluid dynamics methods to improve computational efficiency while maintaining accuracy.¹⁶ All coronary CTA scans were quality checked by HeartFlow to assess eligibility for FFR_{CT} analysis. Cases with severe image artifacts (i.e., noise, blooming, motion, and misalignment) hampering analysis and cases in which the myocardium or coronary arteries were partly outside the field of view were rejected for analysis. Current FFR_{CT} technology is not validated for the calculation of values below 0.50, given the limited number of patients with invasive FFR below 0.50 in the validation phase of FFR_{CT}. Therefore, occluded vessels and vessels with an FFR_{CT} < 0.50 were assigned a value of 0.50.

2.4 | FFR_{CT} planner analysis

A researcher blinded to invasive FFR measurement aligned the location of FFR_{CT} measurement and the modification of coronary stenosis on

FFR_{CT} planner with the location of invasive FFR measurement and actual stent implantation performed by the interventionalist during PCI in a computational model to determine the corresponding FFR_{CT} value and the FFR_{CT} planner value (Figure 1). This process was performed to ensure that the modification of stenosis on the FFR_{CT} planner tool matched the stent length and location actually performed by the interventional cardiologist in that particular case. For FFR_{CT} planner computation, an accelerated method for updating FFR_{CT} is used which is based on a reduced order model derived from computational fluid dynamics. The idealized vessel lumen dimensions are calculated by evaluating the stenosis and subsequently calculating the dimensions in which there would be no lumen narrowing using the idealized vessel algorithm. This algorithm uses a monotonic radius optimization to compute a radius value along the entire length of the vessel, from the ostium to the most distal vessel outlet. This model fits closely to the original lumen, but requires that the radius can only decrease in value going from proximal to distal. Finally, to enable real time computation, a computational fluid dynamics reduced order model is used to calculate

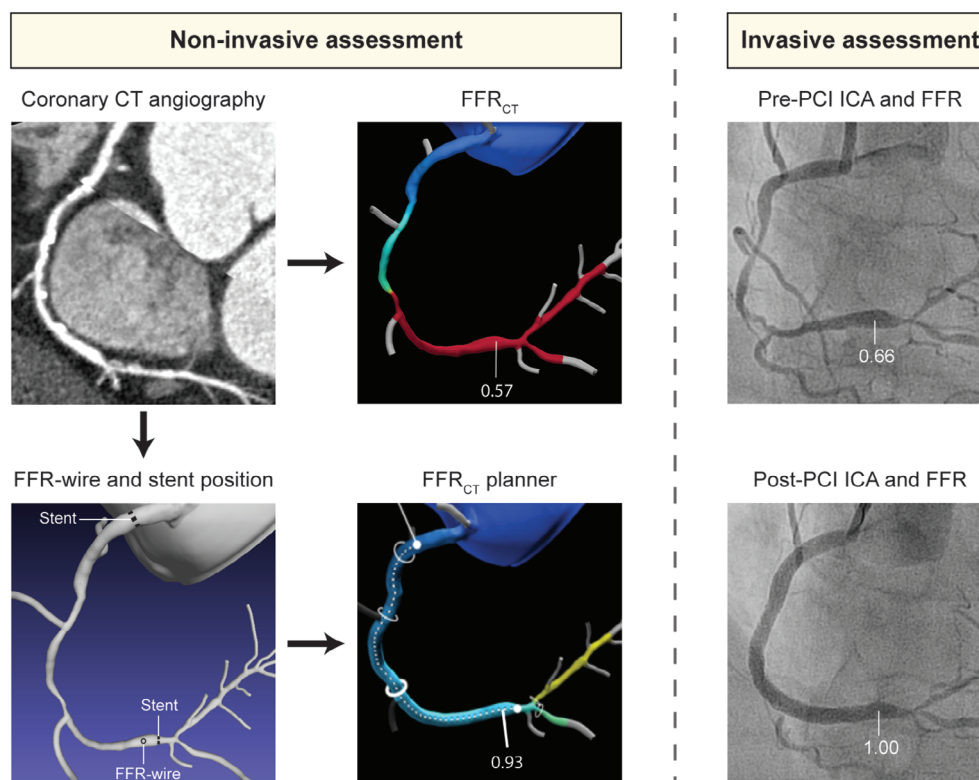


FIGURE 1 Case example of non-invasive assessment with FFR_{CT} and FFR_{CT} planner and invasive assessment with ICA and FFR in a patient undergoing revascularization. Non-invasive coronary computed tomography (CT) angiography showed diffuse disease in the RCA, with multiple severe stenoses along the course of the vessel. FFR_{CT} derived from standard coronary CT angiography images was calculated to be 0.57 in the distal RCA. Invasive assessment pre-PCI confirmed diffuse disease in the mid and distal RCA with a corresponding FFR in the distal RCA of 0.66. Subsequently, PCI was performed with implantation of three stents with a total stent length of 81 mm, resulting in a post-PCI FFR of 1.00. For computation of FFR_{CT} planner, the location of invasive FFR measurement and actual stent location were annotated in a computational model by a researcher blinded to invasive data. After simulation of stenosis removal, FFR_{CT} planner value was shown to 0.93. FFR, fractional flow reserve; FFR_{CT}, computed tomography derived FFR; ICA, invasive coronary angiography; PCI, percutaneous coronary intervention [Color figure can be viewed at wileyonlinelibrary.com]

the FFR_{CT} planner values.¹⁷ In addition to FFR_{CT} and FFR_{CT} planner, delta FFR_{CT} (FFR_{CT} planner - FFR_{CT}) was calculated. Based on previous prognostic invasive FFR data, cut-offs of <0.90 for FFR_{CT} planner³⁻⁵ and < 0.24 for delta FFR_{CT} were used to define failed PCI.⁷

2.5 | Invasive coronary angiography and FFR

ICA and FFR measurements were performed as described previously.¹⁵ ICA was performed using a standard protocol in at least 2 orthogonal directions per evaluated coronary artery segment. For the induction of epicardial coronary vasodilation, 0.2 ml of intracoronary nitroglycerin was administered prior to contrast injection. Lesion length, reference vessel diameter, minimal luminal diameter and percentage diameter stenosis were analyzed using quantitative coronary angiography analysis (CAAS II, Pie Medical, Maastricht, the Netherlands). FFR was measured using a pressure sensor-tipped guidewire (Volcano Corporation, Rancho Cordova, CA). Maximal hyperemia was induced by intracoronary (150 µg) or intravenous (140 µg·kg⁻¹·min⁻¹) administration of adenosine. FFR was calculated as the ratio of mean distal coronary pressure to mean aortic pressure and an FFR of ≤0.80 was considered hemodynamically significant. The choice of revascularization was left to the discretion of the operator and the heart team. In the event of PCI, post-procedural FFR measurements were performed to assess the direct effect of coronary stenting. Care was taken to position the pressure wire tip at the same location as during pre-PCI FFR measurements. All FFR tracings were evaluated by experienced interventional cardiologists blinded to FFR_{CT} findings. In case of significant drift (Pd/Pa at the level of the guiding of >1.02 or < 0.98), FFR measurements were recalculated after correcting Pd.¹⁸ Vessels with a subtotal occlusion in which the operator refrained from obtaining FFR measurement (2 vessels) were assigned an FFR value of 0.50. Additionally, in concordance with FFR_{CT}, vessels with FFR <0.50 were also assigned a value of 0.50. Delta FFR was calculated as the difference between pre and post PCI FFR (post-PCI FFR - pre-PCI FFR). As in FFR_{CT}, cut-offs of <0.90 post-PCI FFR³⁻⁵ and < 0.24 for delta invasive FFR were used to distinguish between an appropriate and inappropriate hemodynamic result after stenting.⁷

2.6 | Statistical analyses

All statistical analyses were performed using the SPSS software package (version 20.0.0, IBM SPSS Statistics, Armonk, NY), except for receiver operating characteristics (ROC) curve analyses, which were performed with MedCalc for Windows (version 12.7.8.0, MedCalc Software, Oostende, Belgium). Continuous variables were tested for normal distribution. Normal distributed continuous variables are presented as mean ± SD. Non-normal distributed variables are presented as median with interquartile range. The associations between FFR_{CT} (FFR_{CT}, FFR_{CT} planner and delta FFR_{CT}) and invasive FFR (pre-PCI

FFR, post-PCI FFR and delta FFR) were quantified using Spearman's correlation coefficients and agreement was assessed with Bland-Altman analysis and using intraclass correlation coefficients (ICCs) based on a two-way mixed model. To account for clustering of multiple vessel measurements per patient, means of FFR_{CT} (FFR_{CT}, FFR_{CT} planner and delta FFR_{CT}) and invasive FFR (pre-PCI FFR, post-PCI FFR and delta FFR) were compared using a mixed linear model with a fixed effect for the technique and random effects for patient and vessel nested within patient. Receiver-operating characteristic (ROC) curve analysis with calculation of area under the curve (AUC) was performed to investigate the diagnostic value of FFR_{CT} planner for post-PCI FFR <0.90 and the diagnostic value of delta FFR_{CT} for delta FFR <0.24. Subsequently, sensitivity, specificity, positive predictive value, and negative predictive value were calculated. A p-value <.05 was considered statistically significant.

3 | RESULTS

3.1 | Study population

An initial number of 82 patients (95 vessels) were evaluated for inclusion in the current study. Two vessels were excluded from analysis prior to FFR_{CT} analysis; because FFR wire position was not recorded during angiography in one case and because of prior stenting in the target vessel in the other case. Of the 93 vessels submitted for FFR_{CT} analysis, 5 vessels (5%) were rejected after initial image quality check because of motion artifacts in 1 case and misalignment artifacts in 4 cases. Additionally, 8 (9%) vessels were not processed due to technical errors with the FFR_{CT} planner software, that is, merging of two adjacent vessels during computation of idealized lumen dimensions leading to unsuitable models for FFR_{CT} planner computation. The technical rejection rate for FFR_{CT} analysis was therefore 14%. In 17 (18%) vessels, FFR_{CT} analysis was technically possible and completed, however FFR_{CT} values could not be calculated at the same location as invasive FFR measurements due to a vessel diameter < 1.80 mm at the site of measurement (14 vessels) or the presence of a total occlusion on coronary CTA (3 vessels). This resulted in a total study population of 56 patients and 63 vessels. Baseline clinical, angiographic, and procedural characteristics of the 56 included patients are presented in Table 1. The target lesion was most frequently located in the LAD (39 vessels, 62%) and diameter stenosis before and after PCI were 69 ± 13% and 12 ± 9%, respectively.

3.2 | Relationship between FFR_{CT} and invasive FFR

The relationships between FFR_{CT}/FFR_{CT} planner and invasively measured FFR values before and after PCI are illustrated in Figure 2. Pre-PCI, invasive FFR was 0.65 ± 0.12 and FFR_{CT} was 0.64 ± 0.13 ($p = .34$). A significant correlation ($r = 0.53$, $p < .001$, Figure 2(a)) and

TABLE 1 Clinical, angiographic, and procedural characteristics

Clinical characteristics (n = 56 patients)	
Age, years	62 ± 10
Male	47 (84%)
Body mass index	27 ± 3
Diabetes mellitus type II	4 (7%)
Hypertension	25 (45%)
Hyperlipidaemia	28 (50%)
Current tobacco use	5 (9%)
Family history of CAD	28 (50%)
Prior myocardial infarction	7 (13%)
Prior PCI	7 (13%)
Invasive coronary angiography (n = 63 vessels)	
Treated vessel	
LAD	39 (62%)
LCX	8 (13%)
RCA	16 (25%)
Before PCI ^a	
Reference diameter, mm	2.77 ± 0.46
MLD, mm	0.86 ± 0.39
Diameter stenosis, %	69 ± 13
Lesion length	17.1 [11.9–31.0]
After PCI ^a	
Reference diameter, mm	2.83 ± 0.42
MLD, mm	2.49 ± 0.46
Diameter stenosis, %	12 ± 9
Procedural characteristics (n = 63 vessels)	
Stent length, mm	28 [18–38]
Nominal stent diameter, mm	3.32 ± 0.35
Final stent diameter after implantation, mm	3.74 ± 0.44

^aQuantitative coronary analysis.

Abbreviations: CAD, coronary artery disease; MLD, minimal luminal diameter; PCI, percutaneous coronary intervention.

agreement (ICC = 0.50, $p < .001$) were found between pre-PCI FFR and FFR_{CT}. Bland–Altman analysis (Figure 2(b)) showed a mean difference of 0.015 (95% CI: –0.23 to 0.26) between pre-PCI FFR and FFR_{CT}. Post-PCI invasive FFR values were significantly higher than FFR_{CT} planner values (0.89 ± 0.07 vs. 0.85 ± 0.07 , $p < .001$). A significant correlation ($r = 0.41$, $p = .001$, Figure 2(c)) and agreement (ICC = 0.36, $p < .001$) were observed between post-PCI FFR and FFR_{CT} planner. The Bland–Altman plot (Figure 2(d)) showed a mean difference of 0.040 (95% CI: –0.10 to 0.18) between post-PCI FFR and FFR_{CT} planner. Delta invasive FFR and delta FFR_{CT} were 0.23 ± 0.12 and 0.21 ± 0.12 , respectively ($p = .09$). A significant correlation ($r = 0.57$, $p < .001$, Figure 2(e)) was observed between delta invasive FFR and delta FFR_{CT}. Bland–Altman analysis (Figure 2(f)) showed a mean difference of 0.025 (95% CI: –0.20 to 0.25) and a significant agreement was noted between delta invasive FFR and delta FFR_{CT} (ICC = 0.57, $p < .001$).

3.3 | Diagnostic accuracy of FFR_{CT} planner for prediction of FFR and change in FFR after stenting

The diagnostic performance of FFR_{CT} planner for predicting FFR and change in FFR after stenting is listed in the supporting information (Table S1). Accuracy of FFR_{CT} planner <0.90 for post-PCI FFR <0.90 was 62% and accuracy of FFR_{CT} planner for change in FFR, defined by delta invasive FFR of <0.24, was 76%. ROC curve analysis showed moderate diagnostic value of FFR_{CT} planner for post-PCI FFR <0.90 (Supporting information, Figure S1, AUC = 0.70, 95% CI 0.57–0.81). Furthermore, ROC curve analysis showed good diagnostic value of delta FFR_{CT} for delta invasive FFR <0.24 with an AUC of 0.80 (95% CI 0.68–0.89, supporting information, Figure S1).

4 | DISCUSSION

The current study evaluated the performance of the novel non-invasive FFR_{CT} planner tool to predict the hemodynamic gain of PCI. Results show significant albeit modest agreement between FFR_{CT} planner and invasive post-PCI FFR. Additionally, the changes in FFR_{CT} after simulated removal of stenosis demonstrated significant agreement with changes in invasive FFR after PCI. These hypothesis generating results indicate that the FFR_{CT} planner tool may hold promise for the non-invasive prediction of the hemodynamic gain of PCI and for PCI procedural planning. However, given the modest performance of the FFR_{CT} planner tool improvement in technology is warranted before clinical application.

4.1 | Using FFR_{CT} planner to predict post-PCI FFR and changes in FFR after stenting

FFR_{CT} has emerged as a promising non-invasive imaging tool among a myriad of imaging modalities. Recent head-to-head comparisons have shown either comparable or superior diagnostic performance of FFR_{CT} as compared with SPECT, the workhorse in functional imaging of patients with suspected CAD.^{12,19} In addition to the functional assessment of coronary stenoses, recent advances in FFR_{CT} technology have enabled the simulated removal of stenoses hereby predicting the hemodynamic gain of PCI.^{13,20} Kim et al were the first to report on this concept in a small cohort of 44 patients (48 lesions).¹³ Invasive post-PCI FFR and the FFR_{CT} derived values displayed moderate correlation, demonstrating the feasibility of coronary CTA based simulation of stenosis removal. Although these initial findings demonstrated the feasibility of using FFR_{CT} technology to predict post-PCI FFR, these analyses were time consuming and not commercially available. Recent advances however have led to the development of the interactive FFR_{CT} planner tool, which enables physicians to interactively examine the effects of different treatment strategies on FFR_{CT} in real time. The performance of this novel tool was investigated in the present study. Results show significantly lower values for FFR_{CT} planner as compared with invasive post-PCI FFR ($p < .001$), with a

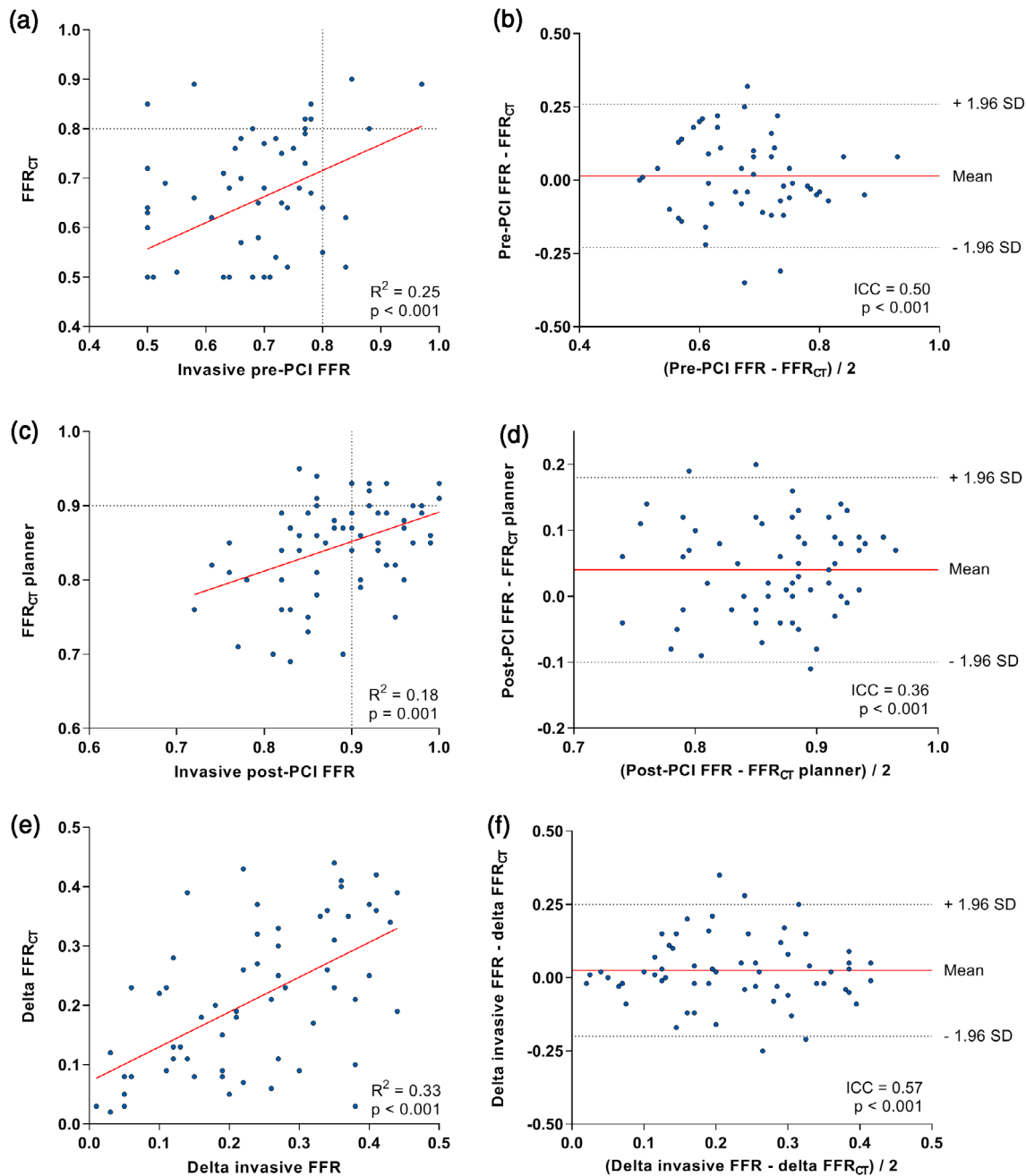


FIGURE 2 Relationship between pre-PCI, post-PCI and delta invasive FFR and FFR_{CT}, FFR_{CT} planner and delta FFR_{CT}. Scatter (a, c, e) and Bland–Altman plots (b, d, f) depicting the relationship between pre-PCI invasive FFR and FFR_{CT} (a, b), between invasive post-PCI FFR and FFR_{CT} planner (c, d) and between delta invasive FFR and delta FFR_{CT} (e, f). FFR, fractional flow reserve; FFR_{CT}, computed tomography derived FFR; ICA, invasive coronary angiography; PCI, percutaneous coronary intervention [Color figure can be viewed at wileyonlinelibrary.com]

mean difference of 0.04. Furthermore, a modest albeit slightly weaker correlation between FFR_{CT} planner and post-PCI FFR was noted in the current report than in the study by Kim et al. Kim et al. subsequently reported a diagnostic accuracy of FFR_{CT} of 96% to predict a post-PCI FFR ≤ 0.80 . Although an FFR value of ≤ 0.80 is established to determine the hemodynamic relevance of stenosis pre-PCI, this cut-off might not be suited for the evaluation of coronary flow after PCI. Since prospective studies on the optimal cut-off for post-PCI FFR are lacking, the optimal threshold to define a satisfactory hemodynamic result of PCI

remains unclear. Retrospective studies have identified different cut-off values ranging from 0.89 to 0.96, with two recent meta-analyses indicated 0.90 as optimal prognostic cut-off for invasive post-PCI FFR.³⁻⁵ Additionally, a recent study has suggested that different cut-off values may apply for non-LAD vessels and LAD vessels.²¹ Despite the limited data on the optimal cut-off for post-PCI FFR, we opted to test the diagnostic accuracy of FFR_{CT} planner for identifying post-PCI FFR of < 0.90 . FFR_{CT} planner demonstrated modest diagnostic performance with an AUC of 0.70 and a diagnostic accuracy of 62%.

In addition to post-PCI FFR values, absolute and relative changes in FFR following stenting have also been associated with cardiovascular events, indicating that prognosis is not solely driven by the final result after PCI but also by the increase in coronary flow following PCI.^{6,7} In the current study, moderate correlation ($r = 0.57$) and agreement ($ICC = 0.57$) were found between delta FFR_{CT} and delta FFR. Furthermore, using a previously described cut-off of 0.24 for invasive delta FFR,⁷ diagnostic performance of delta FFR_{CT} for delta FFR was good with an AUC of 0.80 and an accuracy of 76%. This indicates that the current technology of FFR_{CT} planner may be more useful in predicting the increase in hyperemic pressure changes after PCI than in predicting the absolute post-PCI FFR value. Given the significant albeit modest relationship between FFR_{CT} planner and invasive measurements, the findings from the current proof of principle study may be interpreted as hypothesis-generating, indicating the potential that FFR_{CT} planner holds for non-invasive treatment planning. However, advances in technology are mandatory before clinical application. Furthermore, future large prospective studies are warranted to validate our findings and eventually to test whether FFR_{CT} planner guided PCI may improve clinical outcome as compared with standard-of-care invasive angiography-guided PCI.

4.2 | Non-invasive versus invasive treatment planning

In addition to non-invasive prediction of invasive FFR with FFR_{CT} , recent studies have investigated the use of computational fluid dynamics to compute FFR from ICA to predict the hemodynamic effects of a stenosis.^{22,23} More recently, two studies have investigated novel applications of this technology in which FFR is calculated from ICA after simulation of stenosis removal.^{24,25} Both studies, one using virtual FFR and the other using QFR, have reported good agreement of the computed FFR after simulation of stenosis removal with invasive FFR post-PCI. Notwithstanding these promising results, it is important to note that these technologies are based on ICA and therefore do not allow for patient selection and treatment planning before the invasive procedure. Contrary, non-invasive treatment planning based on coronary CTA is limited by the availability of a sufficient quality coronary CTA scan before PCI and by an inferior resolution as compared with invasive coronary angiography. Further prospective studies are warranted to compare the ability of these promising techniques head-to-head against invasive measurements of FFR to predict the hemodynamic gain after PCI.

4.3 | Potential clinical application of the FFR_{CT} planner tool

Although non-invasive treatment planning using FFR_{CT} planner may help select the most optimal stent size for maximal reduction of lesion-specific ischemia in all cases, treatment planning may be

redundant for experienced PCI operators in non-complex focal lesions with documented ischemia. However, in patients with serial lesions or diffuse disease the FFR_{CT} planner tool may be a useful aid in guiding these more complex PCI procedures. In serial lesions, predicting the hemodynamic effects of stenting individual lesions using invasive FFR is very complex and impractical, requiring balloon dilation of one of the lesion and subsequent wedge pressure measurements.²⁶ Therefore, in clinical practice, interventionalists tend to treat the most severe lesion, either based on angiographic stenosis severity or on the magnitude of the pressure gradient, which may lead to suboptimal stenting. The FFR_{CT} planner tool may assist the operator in these cases to decide between treatment strategies, as illustrated in the case example presented in Figure 3. Modi et al. have recently

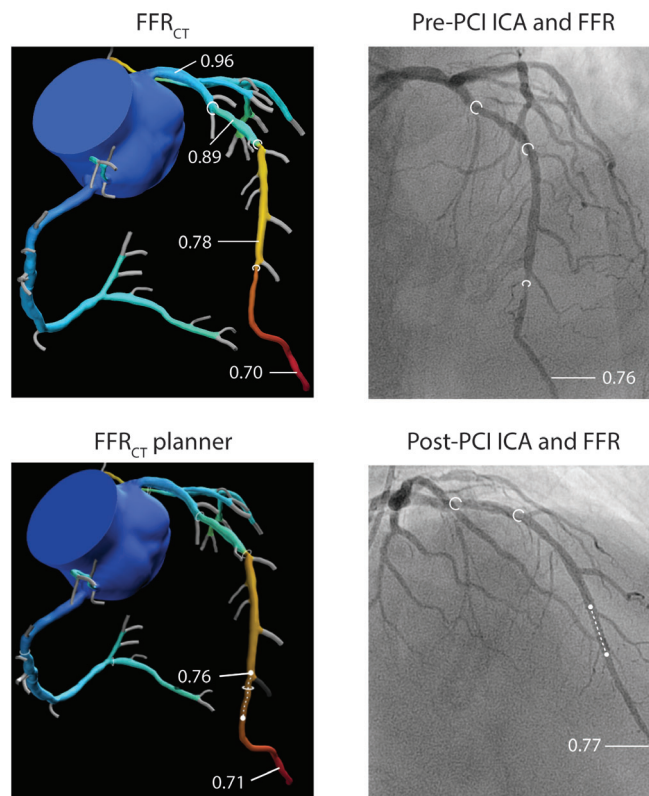


FIGURE 3 Case example illustrating the use of the FFR_{CT} planner tool in a patient with serial stenoses. FFR_{CT} models of coronary CTA and ICA showed serial lesions in the proximal, mid, and distal LAD (stenosis labeled by white circles). FFR_{CT} analysis showed comparable delta FFR_{CT} for the proximal (0.07), mid (0.11), and distal (0.08) lesions, with an FFR_{CT} in the distal LAD of 0.70. Invasive FFR pre-PCI was shown to be 0.76 and since the distal lesions was angiographically most severe, the operator chose to treat the distal LAD. After PCI (stent labeled by white dotted line), there was little increase in FFR (delta FFR of 0.01), with a post-PCI FFR of 0.77. FFR_{CT} planner analysis (stenosis modification labeled by white dotted line) showed comparable results with a delta FFR_{CT} of 0.01 and a FFR_{CT} planner value of 0.71, demonstrating the usefulness of FFR_{CT} planner in treatment planning of serial lesions. FFR, fractional flow reserve; FFR_{CT} , computed tomography derived FFR; ICA, invasive coronary angiography; PCI, percutaneous coronary intervention [Color figure can be viewed at wileyonlinelibrary.com]

highlighted the promise of the FFR_{CT} planner tool to predict the hemodynamic effects of individual stenoses in serial lesions. In a small cohort of 19 vessels, FFR_{CT} planner resulted in improved prediction of residual FFR following stenting of an accompanying serial stenosis as compared with invasive FFR pullback.²⁰ In diffuse disease the hemodynamic gain after PCI is also difficult to predict, with operators often encountering minimal increase in FFR after stenting a focal part of the diffusely diseased vessel. Contrary, as illustrated in the case example presented in Figure 1, stenting from proximal to distal with the use of multiple stents is often needed to achieve a satisfactory hemodynamic result after PCI. The FFR_{CT} planner tool could be useful in these patients to predict the hemodynamic effects of all available stent strategies. However, it is important to note that one should incorporate clinical judgment to avoid excessive stent dimensions, hereby balancing optimal reduction in lesion-specific ischemia limiting and minimization of mechanical complications such as edge dissection. Furthermore, clinical applicability is currently hampered by both the modest performance of the current FFR_{CT} planner tool and the relatively high rejection rate. Improvement in technology is warranted before clinical application.

4.4 | Limitations

This study has several limitations. First, our study is a single-center experience with a relatively small number of patients. Results must therefore be interpreted as hypothesis generating. The international prospective multicenter Precise Percutaneous Coronary Intervention Plan P3 Study is currently ongoing and will test the diagnostic accuracy of FFR_{CT} planner in a large clinical population (NCT03782688). Second, of all initially evaluated cases 14% were rejected for FFR_{CT} planner analysis because of motion artifacts, misalignment, or technical software issues. This is an important limiting factor for the clinical application of FFR_{CT} planner at the current stage of technology. Improvement in technology is warranted to enable clinical applicability. Third, although care was taken to match FFR_{CT} stenosis modification sites to the location of the actual stent implantation, inaccuracies may have occurred. This could have importantly influenced our results. Last, unlike the threshold of 0.80 for pre-PCI which has been extensively validated for clinical events,^{1,27} the thresholds for post-PCI FFR and delta FFR used in the current study are based on retrospective data.^{3-5,7} Further studies are needed to establish the prognostic value of post-PCI and delta FFR. The analyses on the diagnostic accuracy for post-PCI FFR and delta FFR must therefore be interpreted with caution.

5 | CONCLUSION

The novel non-invasive FFR_{CT} planner tool demonstrated significant yet limited agreement with invasive post-PCI FFR values and with changes in FFR values after PCI. These hypothesis generating results indicate that the FFR_{CT} planner tool may hold promise for the non-

invasive prediction of the hemodynamic gain of PCI and for PCI procedural planning. However, given the modest accuracy improvement of the technology is warranted to enable clinical introduction of non-invasive treatment planning.

CONFLICT OF INTEREST

Dr Leipsic has received research grants from GE Healthcare and serves as a consultant and holds stock options in Circle CVI and HeartFlow. Dr Taylor has an equity interest in and is an employee of HeartFlow. Dr Knaapen has received unrestricted research grants from HeartFlow. All other authors have reported that they have no relationships relevant to the contents of this paper to disclose.

ORCID

Roel S. Driessen  <https://orcid.org/0000-0003-3971-0109>

Paul Knaapen  <https://orcid.org/0000-0001-8038-7898>

REFERENCES

1. De Bruyne B, Fearon WF, Pijls NH, et al. Fractional flow reserve-guided PCI for stable coronary artery disease. *N Engl J Med*. 2014; 371:1208-1217.
2. Driessen RS, Danad I, Stuijzand WJ, et al. Impact of revascularization on absolute myocardial blood flow as assessed by serial [(15)O]H₂O positron emission tomography imaging: a comparison with Fractional Flow Reserve. *Circ Cardiovasc Imaging*. 2018;11: e007417.
3. Johnson NP, Toth GG, Lai D, et al. Prognostic value of fractional flow reserve: linking physiologic severity to clinical outcomes. *J Am Coll Cardiol*. 2014;64:1641-1654.
4. Pijls NH, Klauss V, Siebert U, et al. Coronary pressure measurement after stenting predicts adverse events at follow-up: a multicenter registry. *Circulation*. 2002;105:2950-2954.
5. Rimac G, Fearon WF, De Bruyne B, et al. Clinical value of post-percutaneous coronary intervention fractional flow reserve value: a systematic review and meta-analysis. *Am Heart J*. 2017;183:1-9.
6. Lee JM, Hwang D, Choi KH, et al. Prognostic implications of relative increase and final Fractional Flow Reserve in Patients with Stent Implantation. *JACC Cardiovasc Interv*. 2018;11:2099-2109.
7. Fournier S, Ciccarelli G, Toth GG, et al. Association of Improvement in Fractional Flow Reserve with outcomes, including symptomatic relief, after percutaneous coronary intervention. *JAMA Cardiol*. 2019;4: 370-374.
8. Piroth Z, Toth GG, Tonino PAL, et al. Prognostic value of Fractional Flow Reserve measured immediately after drug-eluting Stent implantation. *Circ Cardiovasc Interv*. 2017;10:e005233.
9. Taylor CA, Fonte TA, Min JK. Computational fluid dynamics applied to cardiac computed tomography for noninvasive quantification of fractional flow reserve: scientific basis. *J Am Coll Cardiol*. 2013;61: 2233-2241.
10. Min JK, Leipsic J, Pencina MJ, et al. Diagnostic accuracy of fractional flow reserve from anatomic CT angiography. *JAMA*. 2012;308:1237-1245.
11. Norgaard BL, Leipsic J, Gaur S, et al. Diagnostic performance of non-invasive fractional flow reserve derived from coronary computed tomography angiography in suspected coronary artery disease: the NXT trial (analysis of coronary blood flow using CT angiography: next steps). *J Am Coll Cardiol*. 2014;63:1145-1155.
12. Driessen RS, Danad I, Stuijzand WJ, et al. Comparison of coronary computed tomography angiography, fractional flow reserve, and perfusion imaging for ischemia diagnosis. *J Am Coll Cardiol*. 2019;73: 161-173.

13. Kim KH, Doh JH, Koo BK, et al. A novel noninvasive technology for treatment planning using virtual coronary stenting and computed tomography-derived computed fractional flow reserve. *JACC Cardiovasc Interv.* 2014;7:72-78.
14. Ihdahid AR, White A, Ko B. Assessment of serial coronary stenoses with noninvasive computed tomography-derived Fractional Flow Reserve and treatment planning using a novel virtual stenting application. *JACC Cardiovasc Interv.* 2017;10:e223-e225.
15. Danad I, Rajmakers PG, Driessen RS, et al. Comparison of coronary CT angiography, SPECT, PET, and hybrid imaging for diagnosis of ischemic heart disease determined by Fractional Flow Reserve. *JAMA Cardiol.* 2017;2:1100-1107.
16. LeCun Y, Bengio Y, Hinton G. Deep learning. *Nature.* 2015;521:436-444.
17. Sankaran SLD, Tombropoulos R, Xiao N, et al. Physics driven real-time flow simulations. *Comput Methods Appl Mech Eng.* 2020;364:112963.
18. Pijls NH, Bruyne BD. Fractional Flow Reserve, coronary pressure wires, and drift. *Circ J.* 2016;80:1704-1706.
19. Sand NPR, Veien KT, Nielsen SS, et al. Prospective comparison of FFR derived from coronary CT angiography with SPECT perfusion imaging in stable coronary artery disease: the ReASSESS study. *JACC Cardiovasc Imaging.* 2018;11:1640-1650.
20. Modi BN, Sankaran S, Kim HJ, et al. Predicting the physiological effect of revascularization in serially diseased coronary arteries. *Circ Cardiovasc Interv.* 2019;12:e007577.
21. Hwang D, Lee JM, Lee HJ, et al. Influence of target vessel on prognostic relevance of Fractional Flow Reserve after coronary stenting. *EuroIntervention.* 2019;15:457-464.
22. Morris PD, Ryan D, Morton AC, et al. Virtual fractional flow reserve from coronary angiography: modeling the significance of coronary lesions: results from the VIRTU-1 (VIRTUal Fractional Flow Reserve from coronary angiography) study. *JACC Cardiovasc Interv.* 2013;6:149-157.
23. Xu B, Tu S, Qiao S, et al. Diagnostic accuracy of angiography-based quantitative Flow ratio measurements for online assessment of coronary stenosis. *J Am Coll Cardiol.* 2017;70:3077-3087.
24. Gosling RC, Morris PD, Silva Soto DA, Lawford PV, Hose DR, Gunn JP. Virtual coronary intervention: a treatment planning tool based upon the angiogram. *JACC Cardiovasc Imaging.* 2019;12:865-872.
25. Rubimbura V, Guillon B, Fournier S, et al. Quantitative flow ratio virtual stenting and post stenting correlations to post stenting fractional flow reserve measurements from the DOCTORS (does optical coherence tomography optimize results of stenting) study population. *Catheter Cardiovasc Interv.* 2020;96(6):1145-1153.
26. Pijls NH, De Bruyne B, Bech GJ, et al. Coronary pressure measurement to assess the hemodynamic significance of serial stenoses within one coronary artery: validation in humans. *Circulation.* 2000;102:2371-2377.
27. Pijls NH, van SP, Manoharan G, et al. Percutaneous coronary intervention of functionally nonsignificant stenosis: 5-year follow-up of the DEFER study. *J Am Coll Cardiol.* 2007;49:2105-2111.

SUPPORTING INFORMATION

Additional supporting information may be found online in the Supporting Information section at the end of this article.

How to cite this article: Bom MJ, Schumacher SP, Driessen RS, et al. Non-invasive procedural planning using computed tomography-derived fractional flow reserve. *Catheter Cardiovasc Interv.* 2021;97:614-622. <https://doi.org/10.1002/ccd.29210>